Biophysical Journal, Volume *119*

Supplemental Information

Binding Dynamics of α-Actinin-4 in Dependence of Actin Cortex Tension

Kamran Hosseini, Leon Sbosny, Ina Poser, and Elisabeth Fischer-Friedrich

Supporting material:
Binding dynamics of alpha-actinin-4 in dependence of actin cortex tension

K. Hosseini,[1,2] L. Sbosny,[2] I. Poser,[3] and E. Fischer-Friedrich[1,2,a)]
[1)] *Cluster of Excellence Physics of Life, Technische Universität Dresden, Dresden, Germany*
[2)] *Biotechnology Center, Technische Universität Dresden, Dresden, Germany*
[3)] *Max-Planck-Institut für Zellbiologie und Genetik, Pfotenhauerstraße 108, 01307 Dresden, Germany*

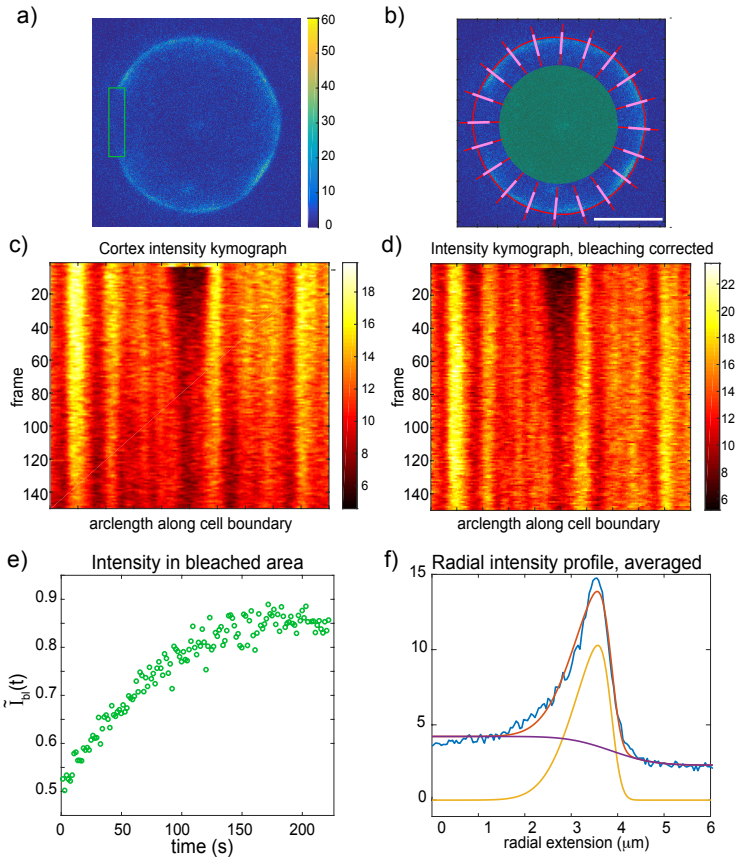

Figure S1. Exemplary analysis of photo-bleaching recovery in a mitotic HeLa cell with mKate2-labeled α-actinin-4. a) Confocal Micrograph of the equatorial cell cross-section right after photo-bleaching. The bleached region is indicated by the green rectangle. b) Same micrograph as in panel a showing now elements for image analysis generated by our analysis code: the identified cell boundary (red cell outline), orthogonal lines to the cell boundary (red and rosa lines, only every tenth line plotted for illustration purposes) and an inner circular cytoplasmic region (green disk) that extends up to 70% of the cell radius. Scale bar: 10 μm. c) Kymograph showing cortical fluorescence over time. Kymographs were generated by plotting integrated fluorescence intensities for each orthogonal rosa line (see panel b) for every time point. d) Kymograph as in panel c but with bleaching correction. Notably, fluorescence intensities outside the bleached region now remain constant on average. e) Averaged and normalised fluorescence intensity over time in the bleached region of the cortex (see panel a). Intensity values were corrected for photo-bleaching. f) Fluorescence intensity profile averaged along the cell circumference before photo-bleaching (blue curve). A smoother version of the fluorescence profile is obtained by fitting the function given in Equation (1), main text (red curve), which consists of a cortical skewed Gaussian (yellow curve) and a contribution that captures cytoplasmic and background fluorescence (violet curve).

[a)] Electronic mail: Corresponding author: elisabeth.fischer-friedrich@tu-dresden.de

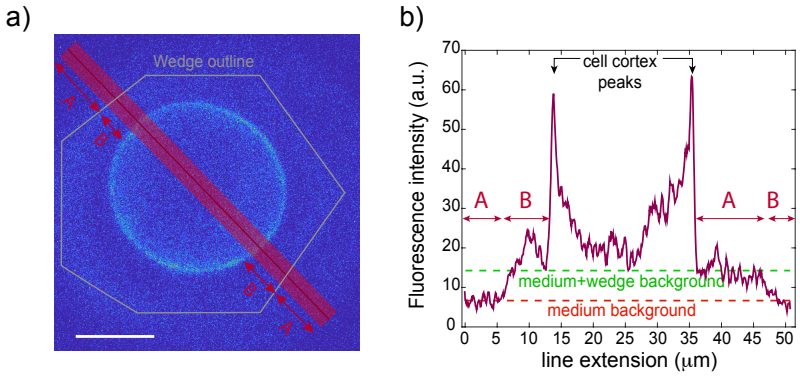

Figure S2. Quantification of background fluorescence from the cantilever wedge. a) Exemplary picture of fluorescence profile of the equatorial cross-section of the cell with surrounding. The cantilever wedge (indicated by the grey outline) is a source of autofluorescence. Scale bar: 10 μm. b) A line scan across the cell shows the fluorescence profiles in three different areas: outside the cantilever wedge area (A), underneath the cantilever wedge but outside the cell (B), underneath the cantilever wedge inside the cell (central region). Inside area A, fluorescence stems from autofluorescence of the medium. Inside area B, fluorescence emanates from autofluorescence of the medium and the wedge. Inside the central region, fluorescence stems from fluorescence of cellular components and autofluorescence of the wedge.

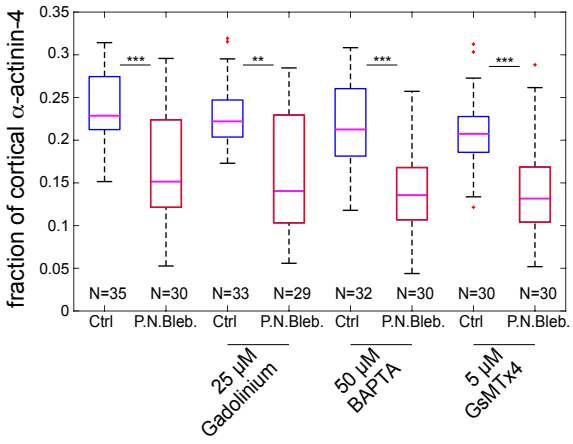

Figure S3. Estimated fractions of cortical α-actinin-4 in the mitotic cortex of HeLa cells expressing Actn4-EGFP in the presence of ion channel inhibitors: 25 μM Gadolinium chlroide (stretch-sensitive membrane channels inhibitor), 50 μM BAPTA (calcium chelator) and 5 μM GsMTx4 (Piezo1 inhibitor) were used in control conditions as well as pharmacologically tension-reduced conditions (incubated with 10 μM Para-Nitro-Blebbistatin, shown in red). This shows conserved reduction of cortical fraction of α-actinin-4 in tension-reduced conditions upon inhibition of calcium, mechanosensitive or stretch-activated ion channels. In conclusion, also in the presence of inhibited ion channel activity, α-actinin-4 binds the cortex at a higher affinity in conditions of high cortical tension as compared to tension-reduced conditions (10 μM Para-Nitro-Blebbistatin).

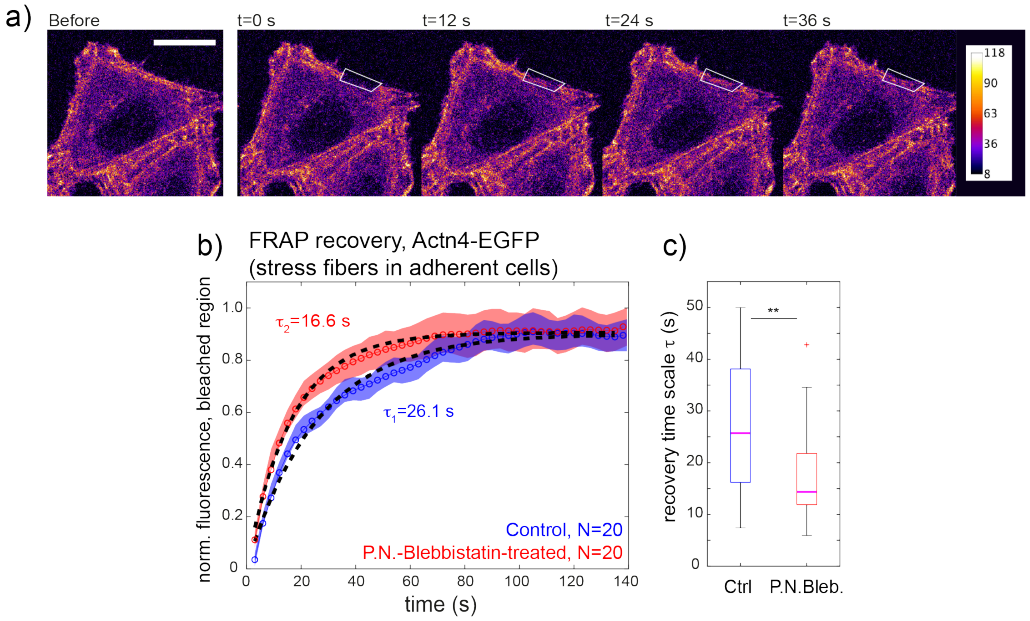

Figure S4. Photo-bleaching of α-actinin-4 in stress fibers of adherent HeLa cells expressing Actn4-EGFP. a) Exemplary confocal image time series of photo-bleaching. The bleached region was indicated by a white boundary. Scale bar: 20 μm. b) Averaged recovery curves of normalized fluorescence intensity in control conditions (N=20, blue curve) and of cells with pharmacologically reduced cortical tension (N=20, red curve, incubated with Para-Nitro-Blebbistatin at 10 μM). Red and blue shaded regions indicate the respective standard error of the mean for each condition. Averaged normalized curves were fitted with an exponential increase (black dashed lines), with fit time scales of τ = 26.1 s (control) and 16.6 s (P.N.Bleb., 10 μM). Fluorescence was not corrected for bleaching. c) Recovery times from fits of individual recovery curves in control and Blebbistatin-treated conditions corresponding to b.

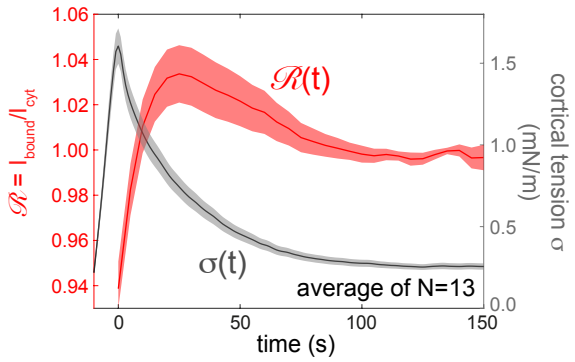

Figure S5. Cell-squishing experiment in the presence of 25 μM Gadolinium chloride (stretch-sensitive membrane channels inhibitor) analogous to Fig. 4, main text. Shown are the averaged time evolution of cortical tension (grey curve) and the normalised α-actinin-4 fluorescence at the cortex (red curve) during and after mechanical squishing of the cell. Averages were taken over 13 cells. Red and grey shaded regions indicate the respective standard error of the mean for cortex/cytoplasm ratio and tension, respectively. Cells were mechanically perturbed by a fast lowering of the AFM cantilever onto the cell (see Materials and Methods). Thereby, a mechanical stretch of cortical area was induced. Cells were in mitotic arrest and, in addition, treated with the ROCK inhibitor Y27632 (5 μM). ROCK inhibition was necessary to avoid blebbing during mechanical cell squishing. In conclusion, also in the presence of an inhibitor of stretch-sensitive membrane channels, cortical association of α-actinin-4 peaks shortly after mechanically induced tension peaks.

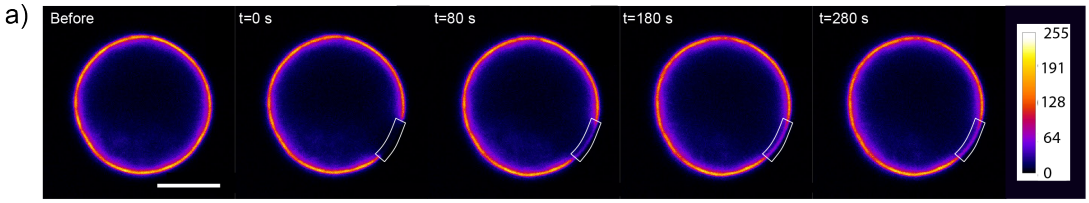

Figure S6. Exemplary photo-bleaching of the K255E mutant of α-actinin-4 in the mitotic cortex. The cell was compressed by the wedged cantilever of an AFM and the equatorial plane was imaged. The bleached region was indicated by a white boundary. Scale bar: 10 μm.

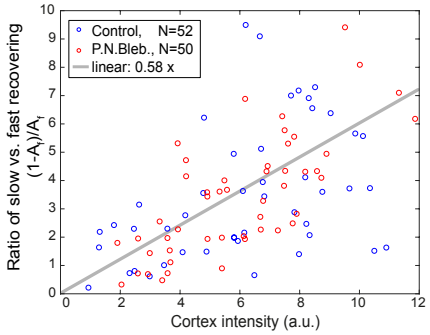

Figure S7. Ratio of slow versus fast recovering fractions in dependence of absolute cortical fluorescence intensities (same data as panel Fig. 7f, main text). The Pearson correlation coefficient was determined as 0.43 with a p-value of $\approx 10^{-5}$ (data points of both conditions were pooled).

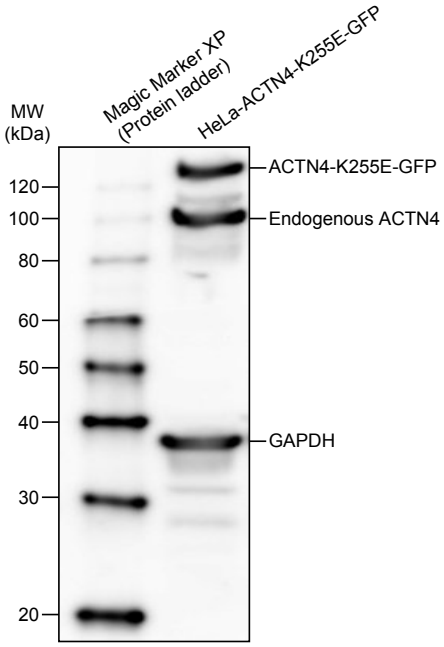

Figure S8. Western blots from whole cell lysate of HeLa cells transfected with a plasmid expressing ACTN4-K255E-GFP. The ratio of endogenous to mutant ACTN4 was 1:0.7 according to the blot. The fraction of K255E transfected cells was approximately 27 %. Therefore, we estimate that transfected cells contain on average have about 2.6 times more mutant protein than endogenous protein. Blots were prepared and quantified as described previously[1].

REFERENCES

[1]Hosseini K, Taubenberger A, Werner C, Fischer-Friedrich E (2019) EMT-induced cell mechanical changes enhance mitotic rounding strength. bioRxiv p. 598052.